GEOACTA, 23, 51-65,1998

RESIDUAL FLUXES OF MASS, SALT AND SUSPENDED SEDIMENT THROUGH A SECTION OF THE BAHIA BLANCA ESTUARY

Daniel E. Pérez [1,2] and Gerardo M. E Perillo[1,3]
[1] Instituto Argentino de Oceanografía, CC 107, 8000 Bahía Blanca
[2] Depto. de Ingeniería, Universidad Nacional del Sur, Av. Alem 1253, 8000 Bahía Blanca
[3] Depto. de Geología, Universidad Nacional del Sur, San Juan 670, 8000 Bahía Blanca

ABSTRACT

Observations of currents, salinity, suspended load for a section of the Bahía Blanca estuary are presented and the residual fluxes of these variables are estimated. The variables were measured at two stations over a complete spring tidal cycle. Data are analyzed employing a proportional grid which provided the residual fluxes and the Euler and Lagrangean residual currents and Stokes drift. The cross-section is partly mixed but there is a significative amount of water entering the Principal Channel from the southern tidal flats during ebb.

RESUMEN

Se presentan observaciones de corrientes, salinidad, y sedimentos en suspensión para una sección del estuario de Bahía Blanca complementado con la estimación de los flujos residuales de dichas variables. Las mismas fueron obtenidas en dos estaciones durante un ciclo completo de marea de sicigias. Los datos fueron interpolados a una grilla proporcional que permite luego calcular los flujos residuales y flujos de Euler y Stokes. Los resultados muestran una sección de mezcla parcial con un significativo ingreso de agua proveniente de las planicies de marea durante el reflujo

1. INTRODUCTION

Bahía Blanca Estuary is situated in the south west of Buenos Aires province, Argentina (Fig. 1). The estuary is the second largest coastal system in the country formed by a series of NW-SE trending major tidal channels that separate extensive tidal flats, low marshes and islands. Along the northernmost channel, Principal Channel, a series of harbors cover a wide variety of economic (Puerto Galván, Ingeniero White, Puerto Rosales, etc) and military activities (Puerto Belgrano).The Principal Channel has been recently dredged to 45 feet depth, making Ingeniero White the deepest port in the country. Maintenance dredging is permanent by now.

Due to the presence of the tidal flats and the mesotidal conditions, the circulation in the estuary in general, and in the Principal Channel, in particular, is very complex. Industrial activity plus increasing urban development pose a threat of pollution. Therefore, knowledge of residual circulation becomes essential to determine the fate of

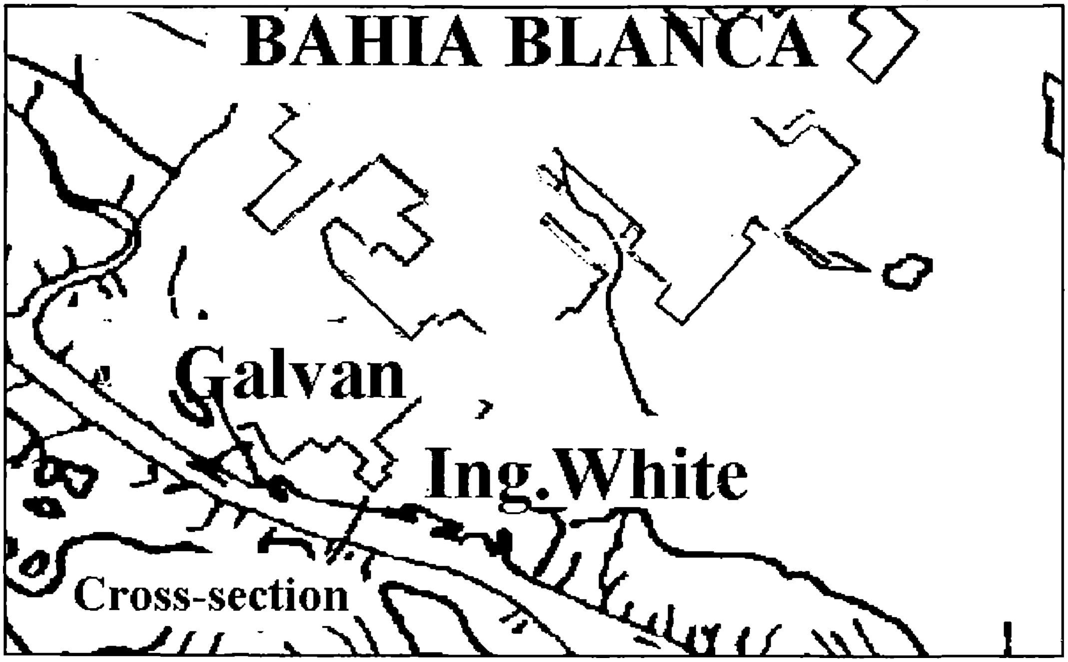

Figure 1. Location map of the inner Bahía Blanca estuary. The study was concentrated in the Principal Channel between Ing. White and Galván Harbors. The southern coast is a tidal flat.

any contaminant. Then, the present study is a contribution to the general understanding of the most active portion of the estuary

The head of the estuary has very little fresh water input. Only the Sauce Chico River enters the estuary near its head providing, on average, less than 5 m^3 s^{-1} water discharge. The southern coast is mostly formed by tidal flats with a dense network of tidal channels which connect the studied area with the southernmost part of the estuary, configuring an open system. This characteristic determines a non-linear system and residual (tidal averaged) fluxes reflect the general situation of this portion of the estuary.

The geomorphology and general circulation of the estuary has been described by Perillo and Piccolo (1999). Our study is directly related to a cross-section located near Ingeniero White harbor in a rectilinear portion of the Principal Channel. The area was studied from the geomorphological and sediment transport point of view by Perillo and Sequeira (1989), the general physical oceanographic conditions (Piccolo and Perillo, 1990) and from its geomorphologic and sedimentologic characteristics by Gómez *et al.* (1997). Therefore, the objective of this paper is to describe the behavior of the residual fluxes of salt, mass and suspended sediments in a specific cross-section of the Principal Channel to define the possible mechanisms that induce such deviation in the circulation.

2. METHODOLOGY

A field cruise was carried out on October 3, 1996 on a cross-section perpendicular to the channel, near Ingeniero White harbor (Fig. 1). Velocity, conductivity, temperature and suspended sediment concentration were measured at two stations, previously positioned by GPS (Fig 2) following the methodology devised by Perillo and Piccolo (1993) for one boat and one set of instruments. The shape of the cross-section was determined by an echosounder and the stations were marked with buoys and anchors. The normal seaward direction to the section had an azimuth of 134° as it is used to correct the current directions.

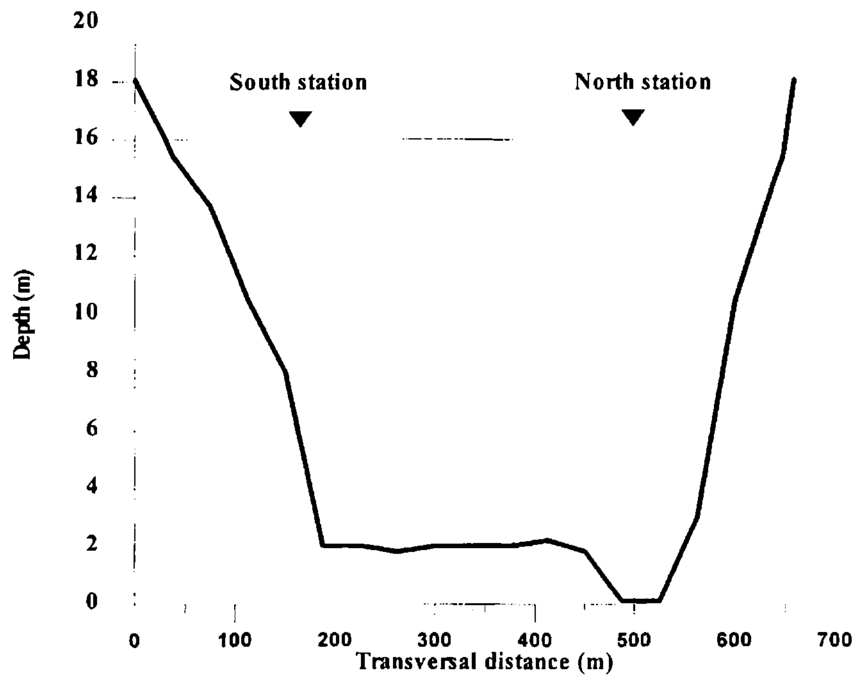

Figure 2. Profile of the cross-section studied. This section has been dredged and is under a heavy traffic. Average depth is 15.9 m and the corresponding surface length is 650 m.

Velocity profiles were obtained every 40 minutes alternating the two stations. They were measured using a Valeport currentmeter, at five levels at every station but following a logarithmic distribution. The different positions of the currentmeter were determined in function of the depth found at the station. Conductivity and temperature profiles were obtained at every station with a Mini CTD InterOcean. The instrument was lowered and raised while data was logged every 10 s on a computer. Suspended sediments were measured by a Kahlsico optical nephelometer based on light transmittance in the water. Suspended sediments profiles were obtained at one-meter intervals at each station. Tidal height was registered by the tidal gauge from Dirección Nacional de Construcciones Portuarias y Vías Navegables (DNCPVN) (Fig. 3).

Data reduction also followed the methodology developed by Perillo and Piccolo (1993) to convert data sampled at irregular space and time intervals into a pseudosynoptic data array. The method is briefly described here. First, flow velocities are decomposed into a component parallel to the channel axis (u) positive in the ebb direction and another normal to it (v) positive to the right. Data at five non-dimensional levels $\eta = 0.1$ (0.2) ... (0.9) at 1 hour intervals were obtained by interpolation using the Stineman algorithm (Perillo and Piccolo, 1991).

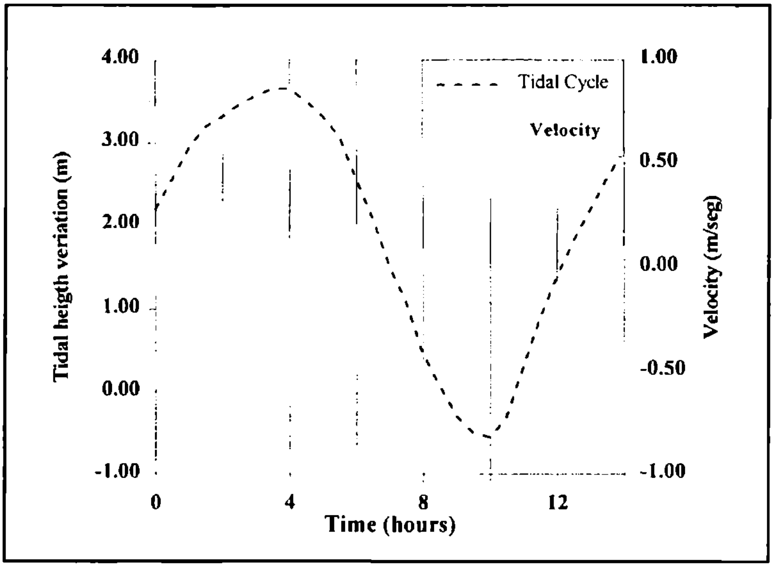

Figure 3. Tidal elevation at the DNCPVN gauge on the left and velocity measured at the cross-section on the right, versus time in hours from the beginning of the measurement period at 0800 h, October 3, 1990.

A similar procedure is followed for the other variables. Therefore, a set of five tridimensional matrices of five rows, three columns, and 13 time intervals are obtained after the reduction. To obtain the fluxes of water (Q), salt (F), and suspended sediment concentration (B) data were further interpolated to a proportional grid with equal-area cells proposed by Perillo and Piccolo (1993). These authors (1998) demonstrated that this grid is the only possible that does not introduce fictitious errors due to the grid proper.

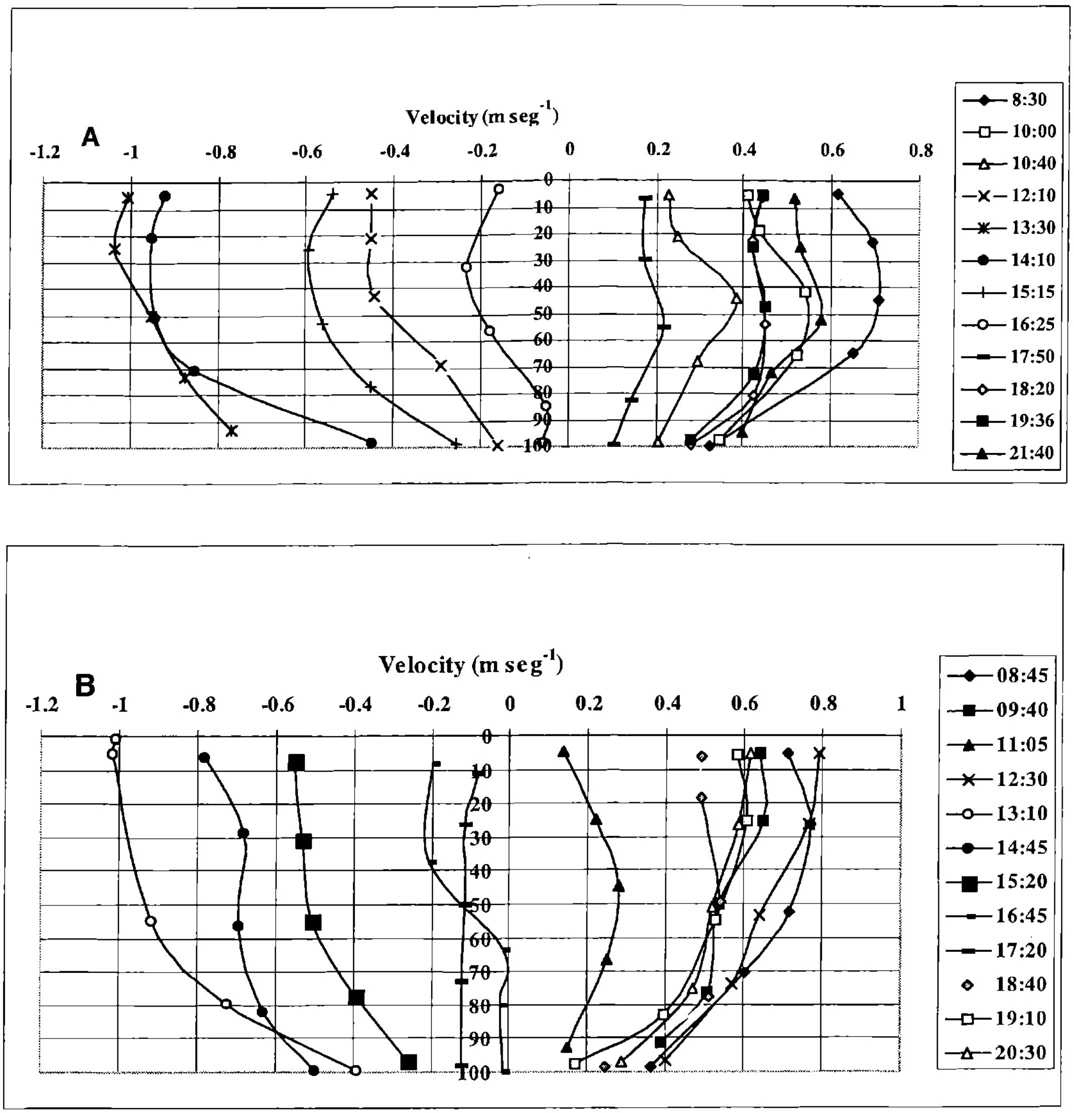

Figure 4. Velocity profiles measured on the a) North and b) South stations versus their relative depth. Positive velocities are ebb-oriented.

Integration over the total tidal cycle gave the net flow of the variables mentioned following the averaging method presented by Kjerfve (1979).

3. RESULTS

The cross-section studied has a rectangular shape with the bottom sloping slightly to the north (Fig. 2). Both walls are steep, specially the northern one, due to dredging. The left side represents the south coast, which is continued by a tidal flat that permits the entrance of water from other parts of the estuary when flooded. The average depth for the section is 15.9 m and the corresponding cross-section width is 650 m, both considered at the Datum Plane level.

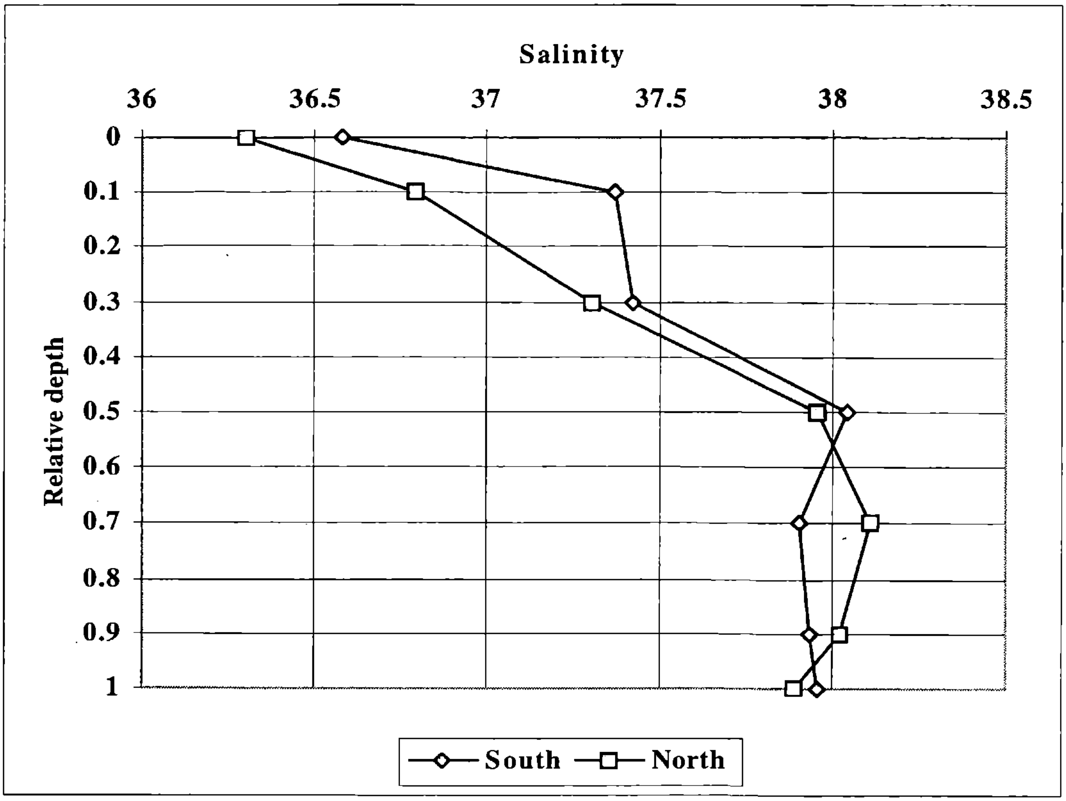

Figure 5. Salinity profiles averaged over the total tidal cycle. South station denotes a high value at relative depth 0.1 due to the high salt content water coming into the channel over the tidal flats. Note the salinity range in analyzing the vertical structure of the water column.

During the study period tidal amplitude was 4.2 m corresponding to extreme spring conditions (Fig. 3). The cross-section averaged longitudinal current velocity (U) was asymmetric in the velocity curve (Fig. 3). The flood lasted 5 hours while de ebb is 7 hours long. On the other hand, the flood had larger velocities. The maximum velocities measured during the ebb were 0.69 m s^{-1} and 0.77 m s^{-1} for North and South stations, respectively. Again the maximum velocities for the flood were 1.04 m s^{-1} and 1.17 m s^{-1} for North and South stations, respectively.

Velocity profiles for each station (Fig. 4a,b) show a nearly logarithmic distribution but with some examples of acceleration and deceleration processes. Thus, maximum velocities occur normally at about 20-40 % below the surface.

On the other hand, average salinity profiles for each station are nearly vertical having as much as 1.8 of salinity stratification indicating a high degree of vertical mixing (Fig. 5) but resulting in partly-mixed conditions. Salinity values are higher than the values found on the continental shelf (Martos and Piccolo, 1988; Cuadrado *et al.* 1999). Obviously there is a concentration mechanism for salt in the middle reach of the estuary where the measurements were done. Piccolo and Perillo (1990) suggested that the higher salinity values may be due to the washing of the salt flat (Salitral de la Vidriera) at the head of the estuary during spring tides. The upper layer on the South Station shows higher salinity values may be due to the input of saltier water from the adjacent tidal flats.

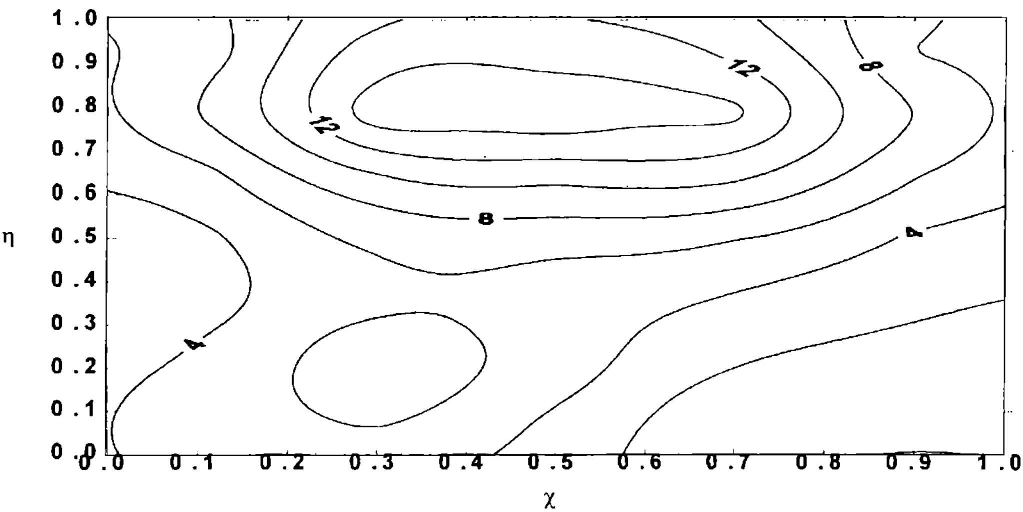

Figure 6. Mass residual flux on the cross-section. Vertical axis is the non-dimensional depth while horizontal axis is the non-dimensional width of the cross section. The flux is seaward in all the section being higher on the center

3.1 Residual fluxes

Estimation of the residual fluxes have been reported in the literature by many authors (Kjerfve *et al.*, 1981; Uncles *et al.*, 1985, Perillo and Piccolo, 1998). A brief description of the method of estimation is outlined here following Perillo and Piccolo (1998). The cross-section area for each time step was divided into 35 cells of equal size. Each cell area (A_{ijk}) is a function of the time. The time period used is k = 1 hour. The values of the longitudinal velocities (U_{ijk}), salinity (S_{ijk}), and suspended sediment concentration (B_{ijk}) were interpolated at the center of each grid cell for each time k. The total amount of mass (Q_{ijk}) over each cell is

$$Q_{ijk} = \rho \, A_{ijk} U_{ijk} \tag{1a}$$

Salt (F), and suspended sediment concentration (C) fluxes going through each cell are calculated using,

$$F_{ijk} = Q_{ijk} S_{ijk} \tag{1b}$$

$$C_{ijk} = Q_{ijk} B_{ijk} \tag{1c}$$

The total residual flux of salt and suspended load averaged over the tidal cycle can be estimated by integrating the areas over the section and time. This operation leads to (Perillo and Piccolo, 1998)

$$\langle F_{vt} \rangle = \langle F_L \rangle + \langle F_{tp} \rangle + \langle F_{vs} \rangle + \langle F_{st} \rangle + \langle F^{*} \rangle \tag{2}$$

$$\langle C_{vt} \rangle = \langle C_L \rangle + \langle C_{tp} \rangle + \langle C_{vs} \rangle + \langle C_{st} \rangle + \langle C^{*} \rangle \tag{3}$$

The <•>means that the term is time averaged over the total tidal cycle. Whereas the terms with subscripts vt are the total number of columns and rows in which the area was divided, terms with subscript L are the rate of transport due to the residual flow of water over the section, with subscript tp are the rate of transport due to the tidal pumping, with subscript vs are due to the vertical shear dispersion, with subscript st are due to the traverse shear dispersion and with superscript * are produced by interaction between vertical and traversal deviations from the mean cross-sectional averages.

According to Uncles *et al.* (1985), mass residual fluxes are estimated from

$$<Q_{vt}> = <Q_s> + <Q_e> \qquad (4)$$

where

$$<Q_s> = <A><\overline{U_s}> \qquad (5)$$

$$<Q_e> = <A><\overline{\overline{U_e}}> \qquad (6)$$

$$<Q_{vt}> = <A><\overline{\overline{U_L}}> \qquad (7)$$

where $<A>$ is the tidal averaged cross-sectional area, $<_s>$ is the mass transport due to the Stokes drift, $<_e>$ is the Eulerian residual current averaged over the section, and $<_L>$ is the sectionally averaged mass (water) transport residual current, also known as Lagrangean residual current.

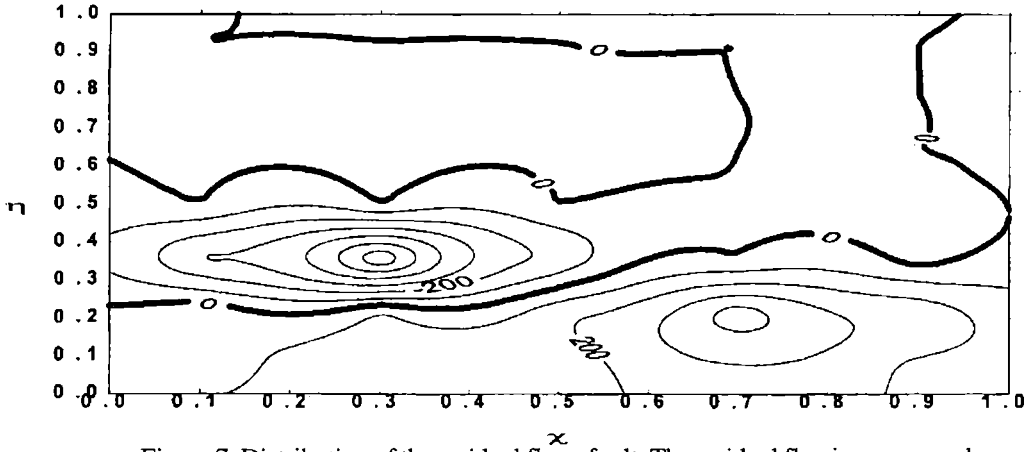

Figure 7. Distribution of the residual flux of salt. The residual flux is very complex developing three flux layers, two within the lower half of the section with reversing directions.

The calculations were done using a proportional grid (Perillo *et al*, 1999).This kind of grid permits to divide the wet area into a number of equal-area cells at the times measurements were made. The method interpolates the tidal depth automatically and calculates the averages of the tidal cycle. The grid is generated regarding the circulation within the area and using the velocity component which is normal to the area considered.

Figure 6 represents a bi-dimensional view of the mass residual fluxes in the cross-section studied. This kind of representation can be done because every averaged area in the section are equal. So the cross-section can be seen as rectangular non-dimensional representation. A seaward residual flux in the whole area is showed on the graph. The Lagrangean, Eulerian and Stokes fluxes are given in Table 1. Although, normally the Stokes terms are negative, in this case they are very small and may be within the error of the instrumentation

Table 1. Residual fluxes and velocities for water mass

Fluxes	Lagrangean	Eulerian	Stokes
$\langle Q \rangle$ ($m^3 s^{-1}$)	6.71	5	1.71
$\langle U \rangle$ ($m\ s^{-1}$)	0.034	0.025	0.009

Salt residual fluxes (Fig. 7) have a completely different pattern to the mass one (compare with Fig. 6). There is clearly a three layer structure and asymmetric with respect to the channel breadth. On the bottom layer and towards the north, the residual flux is seaward, whereas on the middle layer and concentrated to the southern part of the channel the fluxes are headward. Both layers are concentrated within the lower 50 % of the cross-section. The upper layer has flux values very small and vary from positive on the southern portion and negative in the middle and northern sector.

Suspended sediment residual flux has a distribution (Fig. 8) similar to the one observed by the salt flux. A three layer structure and asymmetric with respect to the channel axis. In both cases most of the residual transport occur within the lower half of the cross-section.

Table 2. Estimated residual fluxes for salt (F) and suspended sediments (C) as described in eqs. (2) and (3). Y is a dummy variable representing either F or C.

Fluxes	$\langle Y_{vt} \rangle$	$\langle Y_{L} \rangle$	$\langle Y_{tp} \rangle$	$\langle Y_{vs} \rangle$	$\langle Y_{st} \rangle$	$\langle Y^* \rangle$
F	-22650	4287	17.65	-160.23	-71	-12609
C	-45301	9786	6528	-41193	1483	-33220

The distribution in layers and the lateral variations are clearly evident in the estimated residual fluxes for both variables (Table 2). The total residual flux is headward, but most of the balance is due to both the vertical shear and the interactions that provides most of the landward flux

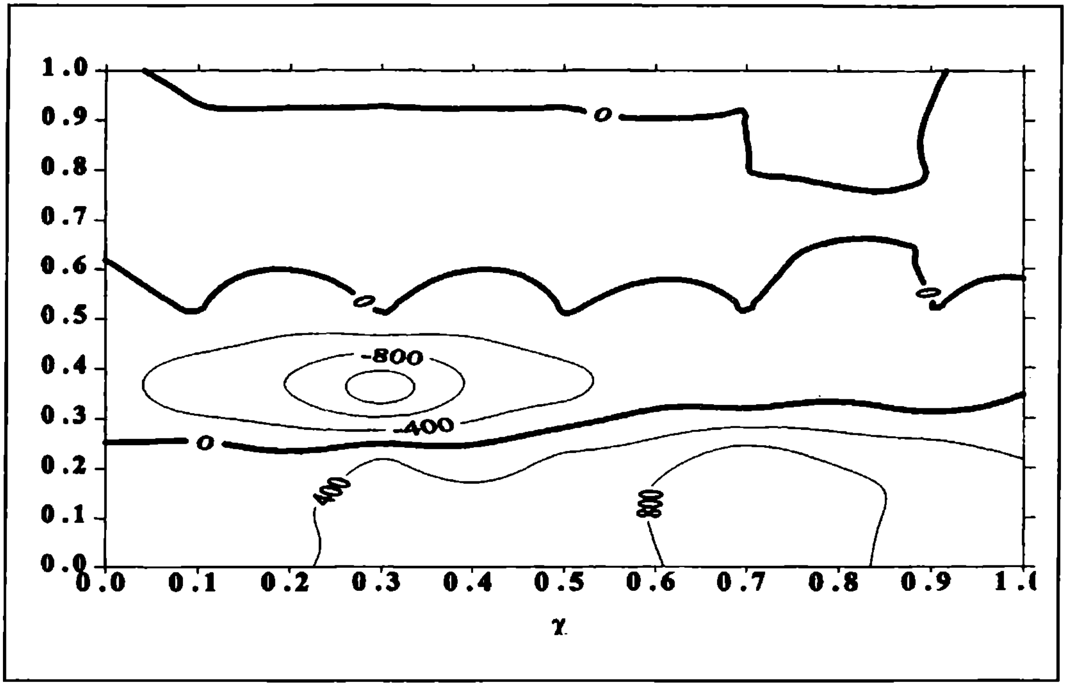

Figure 8. Residual fluxes for the suspended sediment transport at the cross-section. There is an apparent flow of suspended load from southern tidal flats (on the left).

4. DISCUSSION

To illustrate the temporal occurrence of mixing at both stations, the relative contribution of the density gradient and the velocity shear to the bulk Richardson number (Ri) throughout the tidal period was calculated following Dyer and New (1986), In the mixing diagrams the surface-to-bottom salinity difference (ΔS) is plotted against $\bar{u}|\bar{u}|$. According with the specified coordinates $\bar{u}|\bar{u}|< 0$ represents flood conditions. An idealized mixing diagram would show an open anticlockwise hysteresis loop throughout the tidal cycle, in the absence of any mixing (Piccolo and Perillo, 1990). With mixing as well as advection more complicated diagrams occur depending on the degree of mixing and its extent upstream and downstream of the measurement position.

Figure 9 shows the mixing diagram for both stations. The limits of $Ri < 2$ and 20 are presented for the appropriate water depth, assuming that the salinity stratification is directly proportional to the density stratification as was demonstrated by Piccolo and Perillo (1990) for the Bahía Blanca Estuary. Mixing ($2 < Ri < 20$) and well-developed mixing ($Ri < 2$) occurred all the time in the cross-section, being strongest when the currents reach the maximum intensity on the flood or ebb tides.

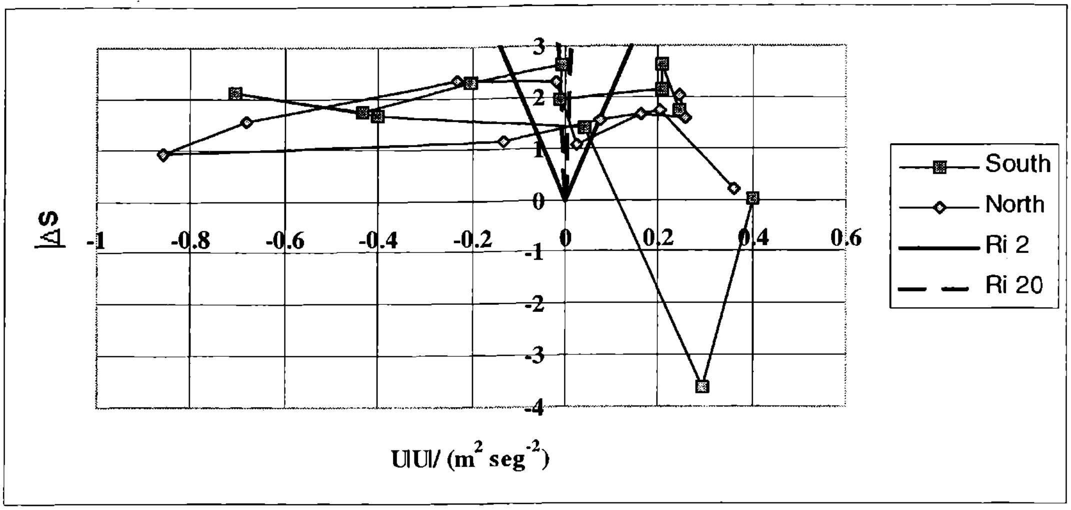

Figure 9. Mixing diagram at the two sections measured. South section present a negative gradient due to the high salt content water coming over the tidal flats. Conditions for stratification were not reached over the cycle measured.

When the S is analyzed, most of the tidal cycle, the gradient was between 1 and 2 salinity units. The gradient was between 2 and 3 at the end of the flooding and during high water slack. Whereas, during ebbing the gradient tended to become less than 1 and even below 0 on station south. The occurrence of such large inverse gradient demonstrate the input of saltier water on the surface. Since this happened during the mid ebb, it is obvious that the water must have come either from the inner estuary or from the adjacent tidal flats.

Salt and suspended sediment concentration fluxes described in Figs. 7 and 8 show patterns significatively different than the one for mass flux. The total mass residual flux is positive whereas both salt and suspended sediment fluxes are negative when the whole section is considered. Most of the ebb-oriented flux is concentrated in the deepest part of the channel over the North side, whereas the reverse fluxes are observed on the southern side (i.e., Fig. 9). A possible explanation is the contribution of saltier water coming into the channel over the tidal flats. High salt content water enter the Principal Channel even when the flood is still pumping sea water into the estuary. This effect can also be seen on Fig. 10 where there are much higher salt values near the surface as detected on the South station during the flood. It is remarkable that we did not detect the same effect in the north station. Near the north coast, the velocities are higher and evacuated more salt than the

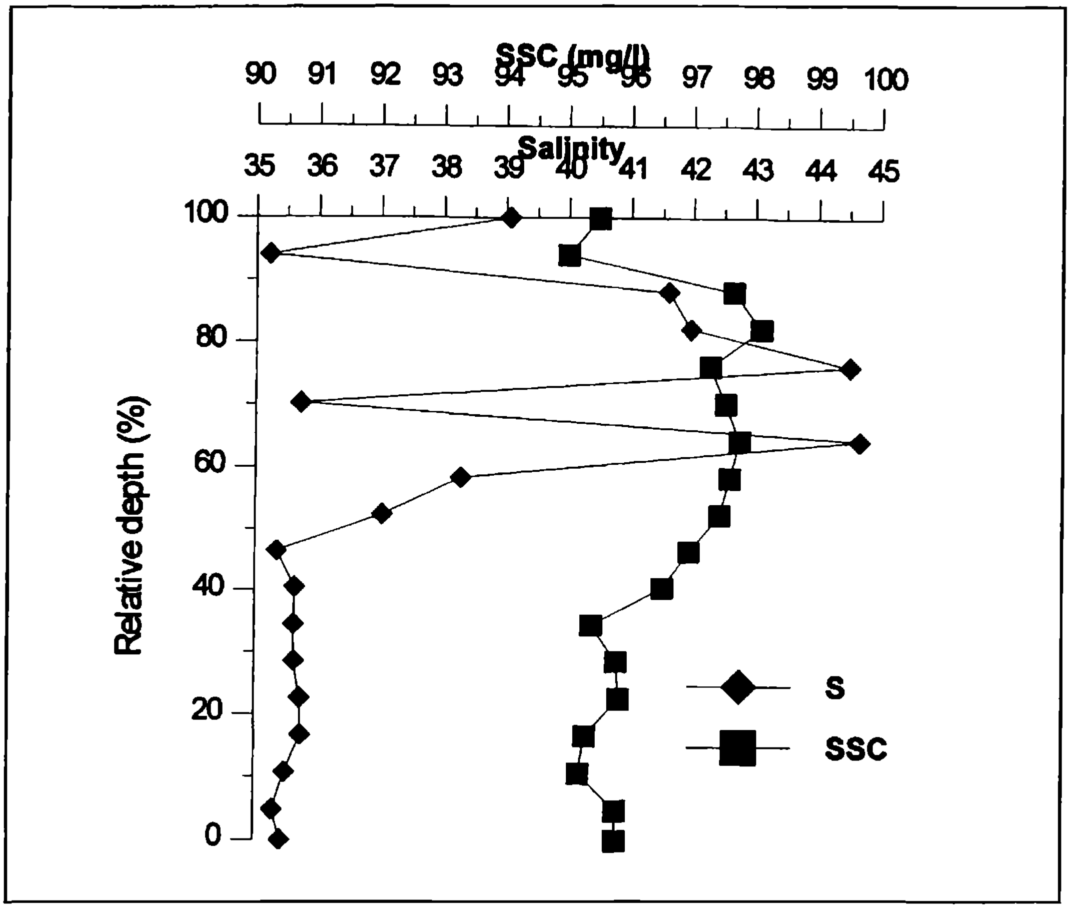

Figure 10. Salinity profile obtained at the South station at 9:35.when the tidal flats were submerged and began to pour water into the Principal Channel. This profile took place during the flood period

one entered during the tidal cycle. Salinity, has put in evidence the circulation system of this area, where the southern tidal flats have a significant influence.

The estimated Lagrangean flux was 6.71 $m^3\ s^{-1}$ directly seaward, a value that should coincide approximately with the runoff inland of the cross-section. Unfortunately, fresh water input was not monitored during the experiment, however, weather conditions were average for the period and no precipitation occurred within 10 d before the study. According to Piccolo *et al.* (1990), the average discharge for the Sauce Chico river, only source of freshwater entering the estuary headward the section considered, is 3.8 $m^3\ s^{-1}$. Lagrangean flow is twice as big as the fresh water input. A difference that can be explained by a surplus of the water entering over the tidal flats from the southern part of the estuary.

The total residual flux for the suspended sediment across the area which is negative (Table 3). During the tidal cycle about five hundred kilograms of suspended sediments entered the head of the estuary. The distribution of the suspended sediment residual flux is shown in Fig 9. There is a concentration of transport headward the estuary near the south section. Also the nucleus of this area is about at 40% of the average height. On the other side, the northern coast, there is a concentration of transport near the bottom (about 10% of the average height), this time seaward. Again the influence of the tidal flats is present now in the suspended sediment transport. Water coming over the tidal flats carries extra amounts of suspended solids which are introduced into the Principal Channel estuary during the flood. Suspended sediment coming from other parts of the estuary over the tidal flats, induce a great distortion in the distribution of suspended sediments residual fluxes, even when there is a high degree of mixing in the area.

6. CONCLUSIONS

A complete tidal cycle has been studied in one of the most active areas in Bahía Blanca Estuary. The data demonstrated that the cross-section behaves as partly mixed. The temperature and salinity profiles are nearly vertical and with only minimum stratification.

The total Lagrangean flux is higher than the possible fresh water input. Although fresh water input was not determined, averages values do not coincide with the Lagrangean flux, denoting an extra source of water which is the flux over the tidal flats all along the south coast of the channel. Tidal pumping effect is very small while the Euler response to it is quite large (four times greater).

Total salt balance results in salt incoming through the section. The distribution of the entering salt in the section considered has a particular shape, which responds to the extra salt flux incoming from the southern tidal flats. High salt content water is transported up during the flood. This explains the peak of incoming residual salt flux on the south coast of the channel.

The distribution of residual flow shows a concentration of incoming suspended sediments near the south coast at 40% of the average depth for the section. This is explained by the incoming flux over the tidal flats during the flood, which is pumpud up through the cross-section studied. On the other hand the north coast reveals a positive (seaward) balance of suspended sediments.

The cross-section studied over a tidal cycle has shown the importance of the incoming water flux over the tidal flats, in water mass, salinity and suspended sediments. The effects of the particular conformation of the system makes necessary to consider the lateral effect of the tidal flats in the circulation of the estuary which exerts a significant influence. A possible way to study this input is defining a cross-section parallel to the southern coast to explore the transversal dynamics on the flats.

7. REFERENCES

Cuadrado, D.G., Piccolo, M.C. and Perillo, G.M.E., 1999. Hydrography of the inner shelf offshore Bahía Blanca Estuary. Continental Shelf Research (in press).

Dyer, K.R. and New, A.L., 1986. Intermitency in estuarine mixing. In: Wolfe, D.A. (ed.) Estuarine variability. Academic Press, New York, pp. 321-339.

Gómez, E.A., Ginsberg, S.S. and Perillo, G.M.E., 1997. Geomorfología y sedimentología de la zona interior del Canal Principal del Estuario de Bahía Blanca. Revista de la Asociación Argentina de Sedimentología 3(2):55-61.

Kjerfve, B., 1979, Measurements and analysis of water current, temperature, salinity and density. In: Estuarine Hydrography and Sedimentation. Dyer K.R. ed. Cambridge University Press, Cambridge, pp 186-226.

Kjerfve, B.; Stevenson, L.H.; Proehl, J.A.; Chrzanowski, T.H. and Kitchens, W.M., 1981.Estimation of material fluxes in an estuarine cross-section: a critical analysis of spatial measurement density and errors. Limnology and Oceanography 26:325-335.

Martos, P. and Piccolo, M.C., 1988. Hydrography of the argentine continental shelf between 38° and 42° S. Continental Shelf Research 8:1043-1056.

Perillo, G.M.E. and Piccolo, M.C. 1991, An interpolation Method for Estuarine and Oceanographic Data. Computers and Geosciences, 17:813-820

Perillo, G.M.E. and Piccolo, M.C., 1993. Methodology to study estuarine cross-section. Revista Geofísica 38:189-206.

Perillo, G.M.E. and Piccolo, M.C., 1998. Importance of grid-cell area in the estimation of the Estuarine Residual Fluxes. Estuaries, 21:14-26

Perillo, G.M.E. and Piccolo, M.C., 1999.- Bahía Blanca Estuary: a review of its geomorphologic and physical characteristics. In: Perillo, G.M.E., Piccolo, M.C. and Pino Quivira, M.(eds.) Estuaries of South America: their geomorphology and dynamics. Environmental Series, Springer-Verlag, Germany (in press)

Perillo, G.M.E., Piccolo, M.C., Mosquera, J. and Aggio, S., 1999. Algorithm to calculate equal-area cells in irregular estuarine cross-sections. Computers & Geosciences (in press)

Perillo, G.M.E. and Sequeira, M.E., 1989. Geomorphologic and sediment transport characteristics of the middle reach of the Bahía Blanca estuary, Argentina. Journal of Geophysical Research-oceans 94:14351-14362

Piccolo, M.C. and Perillo, G.M.E., 1990. Physical characteristics of the Bahía Blanca estuary (Argentina). Estuarine, Coastal and Shelf Sciences 31:303-317.

Piccolo M.C., Perillo G.M.E. and Arango, J.M., 1990. Hidrografía del Estuario del Sauce Chico (Bahía Blanca). Geoacta 17:12-23.

Uncles, R.J., Elliott, R.C.A. and Weston, S.A. 1985. Dispersion of salt and suspended sediments in a partly mixed estuary. Estuaries 3:256-269.